

Reentrant Liquid-Liquid Phase Separation in Protein Solutions at Elevated Hydrostatic Pressures

Johannes Möller,¹ Sebastian Grobelny,² Julian Schulze,¹ Steffen Bieder,¹ Andre Steffen,¹ Mirko Erklamp,² Michael Paulus,¹ Metin Tolan,¹ and Roland Winter²

¹Fakultät Physik/DELTA, TU Dortmund, 44221 Dortmund, Germany

²Physikalische Chemie, Fakultät für Chemie und Chemische Biologie, TU Dortmund, Otto-Hahn Strasse 6, 44227 Dortmund, Germany

(Received 6 September 2013; published 14 January 2014)

We present results from small-angle x-ray scattering data on the effect of high pressure on the phase behavior of dense lysozyme solutions in the liquid-liquid phase separation region, and characterize the underlying intermolecular protein-protein interactions as a function of temperature and pressure in this region of phase space. A reentrant liquid-liquid phase separation region has been discovered at elevated pressures, which originates in the pressure dependence of the solvent-mediated protein-protein interactions.

DOI: 10.1103/PhysRevLett.112.028101

PACS numbers: 87.15.km, 61.05.cf, 81.40.Vw, 87.15.Zg

Understanding of the phase behavior of dense protein solutions is of fundamental importance in various fields of research. For example, protein aggregation and phase separation present the basic mechanisms in diseases such as sickle-cell anemia [1], cataract [2], and conformational diseases such as Alzheimer's or diabetes mellitus type II [3]. In a technological context, knowledge of the phase behavior of proteins is essential in areas such as protein purification and high pressure food processing. A detailed knowledge of the intermolecular interactions and the complete temperature-pressure-concentration phase diagram of proteins would be needed to control and fine-tune proteins' physical-chemical properties, which is especially demanded for the challenging task of protein crystallization [4,5].

The occurrence of a metastable liquid-liquid phase separation (LLPS) region in the phase diagram of proteins has been reported, e.g., for lysozyme [6], γ crystalline [7], and hemoglobin [1] (see Fig. 1). Here, two liquid protein phases coexist, which differ in their protein concentration. Such behavior is generally characteristic for colloidal systems exhibiting strong attractive interactions with a range much shorter than the size of the particles. These solution conditions are typically achieved by screening the repulsive Coulomb interaction with ions [6] or inducing a depletion attraction by crowding agents [8]. Interestingly, the location where the LLPS occurs has been found to foster protein crystallization [6]. Formation of a LLPS in protein solutions has been studied as a function of pH , salt concentration, type of salt, and temperature [6,9–11]. In view of the practical importance and the need for a better understanding of the phase behavior of dense protein solutions, we set out to experimentally explore the effect of high pressure on lysozyme solutions in the vicinity of the LLPS region using small-angle x-ray scattering (SAXS).

Next to temperature and the chemical potentials of solute and solution, pressure constitutes a key variable necessary to develop a complete description of the thermodynamic

behavior of any system, including protein solutions. Pressure offers the advantageous property that it only changes the density of the system. In contrast, a variation in temperature has an impact not only on the density but also on the internal energy of the system. Moreover, pressure is a rather mild perturbing agent and pressure-dependent studies on protein solutions have generally been found to be fully reversible [12–14]. Furthermore, they have been shown to lead to a better understanding of the volumetric and hydrational properties and hence the stability and function of biomolecular systems [12–14]. Nothing is known about pressure effects on the LLPS of dense protein solutions, however.

Lysozyme is known to remain in its native conformation over an extended pressure range, thereby providing the possibility of studying changes of intermolecular interactions over a large range of protein concentrations and pressures [15]. Recently, it has been shown that pressure has an increasing repulsive effect on the intermolecular interaction potential of proteins [15–17], but in the kbar

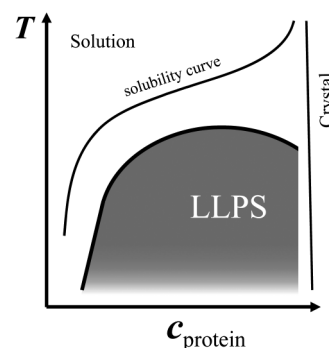


FIG. 1. Schematic temperature-concentration phase diagram of dense protein solutions. A transition to a (metastable) liquid-liquid phase separation region (LLPS) occurs at lower temperatures than the separation between the solution and solid (crystal) phase.

range, this effect is reversed, which has been attributed to changes in the structure of the hydration water [15,18]. This effect was also found to persist at high ionic strengths [19]. Here, SAXS experiments were carried out on lysozyme (14.3 kDa, $pI = 11$, from hen egg white, Roche GmbH, Mannheim, Germany) solutions at various concentrations in the presence of 500 mM NaCl (3 wt.%) and 25 mM of the pressure-stable buffer Bis-Tris (Sigma Aldrich, Steinheim, Germany) [20] at a pH of 7. Before each measurement, lysozyme and salt stock solutions were freshly mixed to obtain final protein concentrations of 18.5, 20.0, and 21.5 wt.% in the presence of 500 mM NaCl, i.e., conditions close to the critical protein concentration of the LLPS region. The SAXS measurements were performed at beam line ID02, ESRF, Grenoble, and beam line I22, Diamond Light Source, Didcot. A custom-built high-pressure cell with two flat diamond windows [21] was used at ID02, a slightly different cell with two sapphire windows [22] at I22. For experimental details see [23].

The SAXS signal of concentrated protein solutions in the decoupling approximation is proportional to the product of the form factor $P(q)$ and the effective structure factor $S_{\text{eff}}(q)$ of the particles. Here, $q = (4\pi/\lambda) \sin(\Theta/2)$ is the wave vector transfer with λ being the wavelength of the incoming beam and Θ the scattering angle. The form factor of the lysozyme molecules was modeled by that of an ellipsoid of revolution with semiaxis $a = 1.52$ nm and radius of gyration $R_g = 1.45$ nm. These values were determined by refining the model to a SAXS curve measured in a diluted lysozyme solution (0.5 wt.%), and are in good agreement with previous investigations [15,19]. The data for the highly concentrated protein solutions exhibit an effective structure factor, which can be described by

$$S_{\text{eff}}(q) = 1 + \frac{\langle F(q) \rangle_{\Omega}^2}{P(q)} (S(q) - 1), \quad (1)$$

where $\langle F(q) \rangle_{\Omega}$ is the spherical average of the Fourier transform of the protein's electron density, and $S(q)$ is the intermolecular structure factor.

For colloidal systems and solution conditions close to a liquid-liquid phase boundary, the intermolecular interaction potential $V(r)$ can be modeled by a sticky hard sphere potential. Here, the potential is described by a hard sphere part, which presents the impenetrable protein surface, and an attractive potential at the protein surface, which is modeled by an infinitesimal narrow, infinitely deep-square well potential [24]:

$$V(r) = \begin{cases} \infty & 0 < r < \sigma \\ \ln(12\tau \frac{\Delta}{\sigma + \Delta}) & \sigma \leq r \leq \sigma + \Delta \\ 0 & \sigma + \Delta < r \end{cases} \quad (2)$$

r is the particle separation and the depth of the well is controlled by the sticking parameter τ , τ^{-1} is a measure of the strength of adhesion, or temperature, respectively. In the limit $\Delta \rightarrow 0$, this so-called Baxter model has an analytical solution for the structure factor in the Percus-Yevick approximation [24]. In order to refine the measured scattering data, the hard sphere diameter of the model was set to $\sigma = 2.9$ nm and the volume fraction φ was calculated from the protein concentration using a density of lysozyme of 1.351 g cm $^{-3}$. Owing to the unknown compressibility data of these dense protein solutions, and the differential compressibilities of the solvent, hydration shell water, and the lysozyme molecules themselves, φ has been kept constant in this rather low pressure range. Maximal increases of a few percent can be expected using bulk water compressibility data, which have been shown to have no significant effect on the refinement of the data, however (see also [23]). The only free parameter to model the scattering data is the stickiness parameter of the attractive part of the interaction potential, which is directly related to the reduced second virial coefficient by [25]

$$b_2 = 1 - 1/(4\tau) \quad (3)$$

The second virial coefficient B_2 , which is often used to describe aggregation and crystallization phenomena, is defined as the second-order parameter of the virial expansion of the osmotic pressure, and is a measure of the integrated strength of particle interactions. By normalizing B_2 to the hard-sphere contribution, B_{HS} , to render it independent of the size of the particle, one obtains $b_2 = B_2/B_{\text{HS}}$ [25]. Negative values of b_2 reveal attractive and positive values dominating repulsive interactions between the molecules. It was found that b_2 displays universal properties for protein solutions. A value of $b_2 < -1.5$ is needed for a protein solution to undergo LLPS [25,26], and a universal crystallization window exists in a certain range of negative b_2 values as well [27].

A typical pressure dependence of the measured effective structure factor $S_{\text{eff}}(q)$ is shown in Fig. 2, together with the refinement of the data. The $S_{\text{eff}}(q)$ data for the 20 wt.% lysozyme solution at 16°C reveal a strong increase of the scattering intensity at low q values upon compression. Note that the sample is in the phase separated state at 1 bar. The highest scattering intensities at small q are observed at pressures of 400 and 2500 bar, respectively, where the sample crosses the phase boundary out of the LLPS into the homogenous one-phase region and vice versa at the higher pressure.

To verify the repeated passage of the phase boundary of the liquid-liquid phase transition, an Ornstein-Zernike analysis of the scattering data has been carried out as well. At near-critical conditions, the scattering intensity should vary approximately as [28]

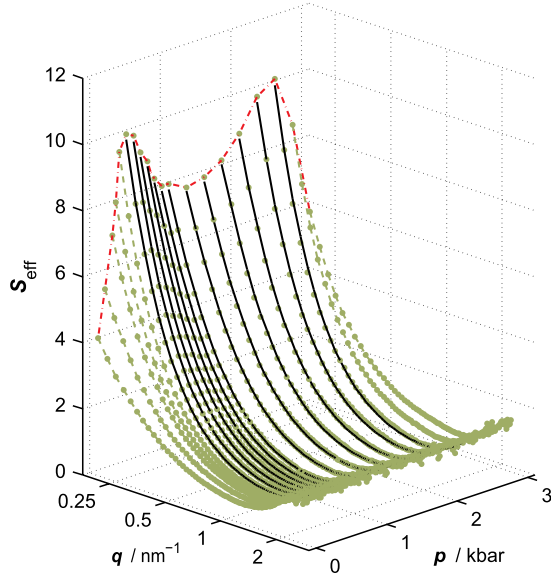


FIG. 2 (color online). Measured effective structure factor $S_{\text{eff}}(q)$ of a 20 wt.% lysozyme solution as a function of pressure at $T = 16^\circ\text{C}$. Black lines display the refinement of the data using the sticky hard sphere model, the red line shows the scattering intensity at $q = 0.2 \text{ nm}^{-1}$ (see also Fig. 3(b)).

$$S(q) = \frac{S(0)}{1 + \xi^2 q^2}, \quad (4)$$

where ξ is the correlation length of density or concentration fluctuations. The refinement to the scattering data can be found in the SI. As an example, Fig. 3(a) displays the pressure dependence of ξ for the 20.0 wt.% lysozyme solution at $T = 16^\circ\text{C}$. A drastic increase of the correlation length is clearly visible when the system passes the LLPS boundary at 400 and 2500 bar, respectively.

The crossing of the phase boundaries is also reflected in the pressure dependence of $S_{\text{eff}}(q)$ at small momentum transfers ($q = 0.2 \text{ nm}^{-1}$), which is shown as the red line in Fig. 2. The complementary data for 8, 20, and 26°C are shown in Fig. 3(b). For reasons of clarity, only four different temperatures are shown. Passing of the phase boundary is indicated by an increase in forward scattering until a certain maximum value is reached (400 bar at 16°C , 1000 bar at 8°C). From there on, the samples are in the homogeneous, one-phase state and show the same nonlinear pressure dependence as the samples at 20°C and 26°C .

To further investigate this effect, the reduced second virial coefficient b_2 , obtained from refinement of the sticky sphere potential to the SAXS data, has been determined for selected highly concentrated lysozyme solutions as a function of temperature and pressure. As an example, Fig. 3(c) displays the pressure dependence of b_2 for the 20 wt.% lysozyme solution. An example of the temperature dependence of b_2 at ambient pressure as well as elevated

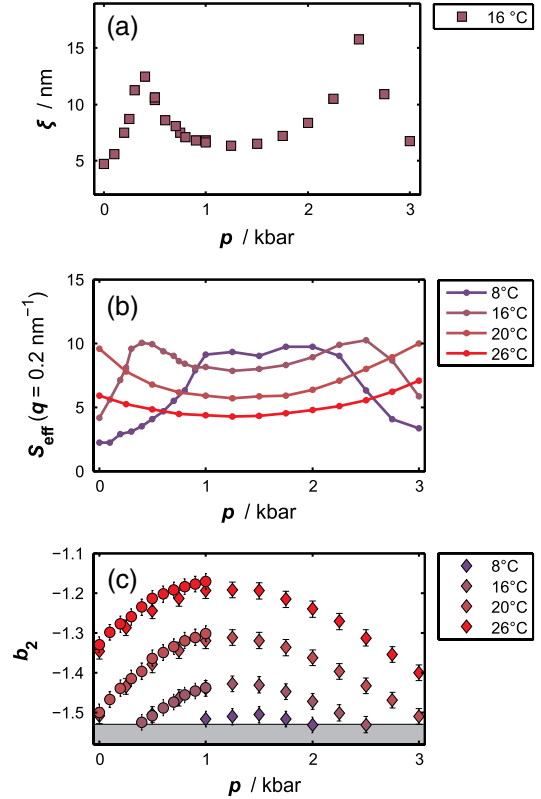


FIG. 3 (color online). (a) Pressure dependence of the correlation length, ξ , for the 20.0 wt.% lysozyme solution at $p\text{H } 7$ and $T = 16^\circ\text{C}$. (b) Pressure dependence of the effective structure factor $S_{\text{eff}}(q)$ at $q = 0.2 \text{ nm}^{-1}$ for 8, 16, 20, and 26°C (top to bottom) (see also Fig. 2). (c) Pressure dependence of the reduced second virial coefficient b_2 obtained from refinement of the SAXS data measured at 8, 16, 20, and 26°C (bottom to top) for a protein concentration of 20 wt.%. The gray area corresponds to solution conditions that exhibit LLPS.

pressures is shown in Fig. 4. For additional data see the Supplemental Material [23].

For conditions where the protein solutions reside in the homogeneous one-phase region, the model to refine the SAXS curves was used to extract numerical values for the reduced second virial coefficient b_2 . As can be seen in Fig. 3(c), $b_2(p)$ nicely reflects the nonlinear pressure dependence of $S_{\text{eff}}(q)$, exhibiting a maximum between 1 and 1.5 kbar. Interestingly, when the protein interactions start to become more attractive again at higher pressures, the system is able to reenter the LLPS regime, which is indicated by a second maximum in $S_{\text{eff}}(q = 0.2 \text{ nm}^{-1})$ at 2.5 kbar for $T = 16^\circ\text{C}$ [Fig. 3(b)]. Furthermore, the values obtained for b_2 are in good agreement with theoretical considerations, predicting the LLPS to occur at about $b_2 = -1.5$ [25,26]. In Fig. 3(c), the phase boundary is marked (gray area: LLPS) at $b_2 = -1.53$ for 20 wt.% lysozyme. Protein samples of 21.5 and 18.5 wt.% show the same behavior (see the Supplemental Material [23]), with similar values for b_2 and slightly different values for the $p - T$

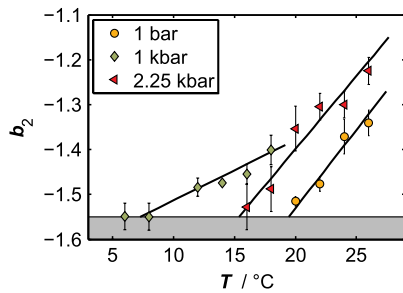


FIG. 4 (color online). Temperature dependence of the reduced second virial coefficient b_2 at pressures of 1 bar, 1 kbar, and 2.25 kbar. The protein concentration is 21.5 wt.%. Black lines indicate a linear fit to assess the LL phase boundary (circles in Fig. 5).

phase boundary of the LLPS (for 21.5 wt.% lysozyme, the phase boundary is found at $b_2 = -1.55$, for 18.5 wt.% at $b_2 = -1.53$).

In addition, we determined the temperature dependence of b_2 at selected pressures. In Fig. 4, b_2 values are shown as a function of temperature at pressures of 1 bar, 1 kbar, and 2.25 kbar, respectively, for a protein concentration of 21.5 wt.%. The data exhibit a linear temperature dependence near the phase boundary for all concentrations and pressures studied. Notably, the temperature dependence is much stronger for the samples at 1 bar and 2.25 kbar, i.e., at conditions where the strength of attractive interactions increases.

From the combined b_2 data, a $p - T$ phase diagram can be constructed for the LLPS region of lysozyme, which is displayed in Fig. 5 for protein concentrations of 18.5, 20.0, and 21.5 wt.%. The data points were obtained from the pressure (diamonds) and temperature (circles) dependent b_2 data. Solution conditions where the samples undergo LLPS are marked in gray. The phase boundary of the LLPS curve

obtained at 1 bar is in good agreement with literature data [9]. As can be clearly seen, a reentrant LLPS is found at high pressures (HP-LLPS) for all protein concentrations studied.

The observed reentrant liquid-liquid phase transition is consistent with the increasing attractivity of the interaction potential $V(r)$ of the dense protein solutions at kbar pressures, which can be explained by a significant change of the water structure, i.e., a collapse of the second water hydration shell (this effect is probably also responsible for the peculiar pressure dependence of the transport properties of water) [15,19]. Notably, this effect has been found to persist also at high salt concentration [19], but can be altered by cosmotropic cosolvents such as trimethylamine-N-oxide, which is known to increase the strength of the hydrogen bonding network of water, thereby counteracting the pressure effect [18].

To summarize, we present results on the effect of high hydrostatic pressure on the phase behavior of dense lysozyme solutions in the liquid-liquid phase separation region, and characterize the intermolecular protein-protein interactions as a function of temperature and pressure in this region of phase space. A reentrant liquid-liquid phase coexistence region has been found at elevated pressures. From the SAXS data in combination with liquid-state theoretical approaches, the strength of the intermolecular protein-protein interactions has been derived, and the pressure dependence of the second virial coefficient could be determined as a function of temperature and pressure. Deciphering the intermolecular interaction potential as a function of temperature, pressure, protein, and salt concentration is essential for understanding protein aggregation and crystallization. As shown in this study, the application of pressure can be used to fine-tune the second virial coefficient of protein solutions, which could be used to tune nucleation rates and hence control protein

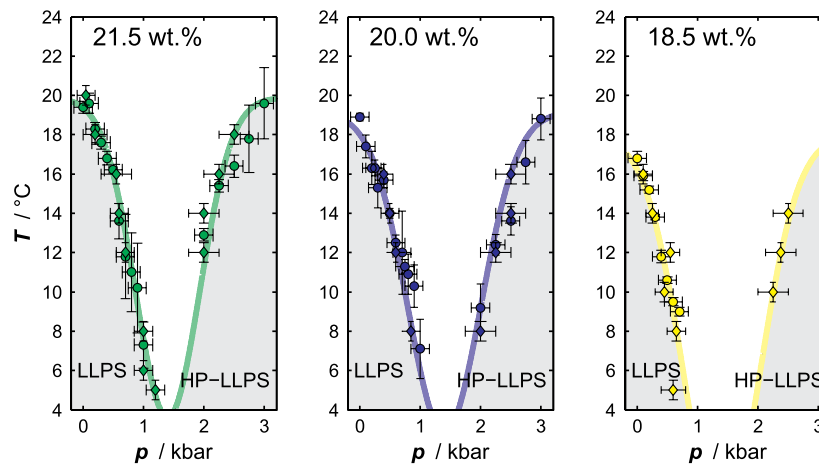


FIG. 5 (color online). $p - T$ phase diagram of the LLPS of lysozyme for concentrations of 21.5, 20.0, and 18.5 wt.%. Low and high pressure (HP) areas of the LLPS are marked in gray. The phase boundaries are refined using a Gaussian function with a center at 1.45 kbar.

crystallization, or to prevent protein aggregation, which might, for example, be of practical importance for long-term storage of concentrated protein solutions.

We acknowledge the European Synchrotron Radiation Facility (ESRF) and the Diamond Light Source for providing synchrotron radiation, and we would like to thank M. Sztucki (ID02), M. Malfois, and A. Smith (I22) for assistance during the beam times. Financial support from the Cluster of Excellence RESOLV (EXC 1069) and FOR 1979 funded by the Deutsche Forschungsgemeinschaft (DFG), the BMBF (05K10PEC), and the NRW-Forschungsschule “Forschung mit Synchrotronstrahlung in den Nano- und Biowissenschaften” is gratefully acknowledged.

-
- [1] O. Glakin, K. Chen, R. L. Nagel, R. E. Hirsch, and P. G. Vekilov, *Proc. Natl. Acad. Sci. U.S.A.* **99**, 8479 (2002).
- [2] A. Pande, J. Pande, N. Asherie, A. Lomakin, O. Ogun, J. King, and G. B. Benedek, *Proc. Natl. Acad. Sci. U.S.A.* **98**, 6116 (2001).
- [3] N. Javid, K. Vogtt, C. Krywka, M. Tolan, and R. Winter, *Phys. Rev. Lett.* **99**, 028101 (2007).
- [4] N. Asherie, *Methods* **34**, 266 (2004).
- [5] R. A. Curtis and L. Lue, *Chem. Eng. Sci.* **61**, 907 (2006).
- [6] M. Muschol and F. Rosenberger, *J. Chem. Phys.* **107**, 1953 (1997).
- [7] J. A. Thomson, P. Schurtenberger, G. M. Thurston, and G. B. Benedek, *Proc. Natl. Acad. Sci. U.S.A.* **84**, 7079 (1987).
- [8] A. Tardieu, F. Bonnete, S. Finet, and D. Vivares, *Acta Crystallogr. Sect. B* **58**, 1549 (2002).
- [9] F. Cardinaux, T. Gibaud, A. Stradner, and P. Schurtenberger, *Phys. Rev. Lett.* **99**, 118301 (2007).
- [10] Y. Zhang and P. S. Cremer, *Proc. Natl. Acad. Sci. U.S.A.* **106**, 15 249 (2009).
- [11] F. Zhang, M. W. A. Skoda, R. M. J. Jacobs, S. Zorn, R. A. Martin, C. M. Martin, G. F. Clark, S. Weggler, A. Hildebrandt, O. Kohlbacher, and F. Schreiber, *Phys. Rev. Lett.* **101**, 148101 (2008).
- [12] K. Heremans and L. Smeller, *Biochim. Biophys. Acta* **1386**, 353 (1998).
- [13] J. L. Silva, D. Foguel, and C. A. Royer, *Trends Biochem. Sci.* **26**, 612 (2001).
- [14] R. Mishra and R. Winter, *Angew. Chem., Int. Ed. Engl.* **47**, 6518 (2008).
- [15] M. A. Schroer, J. Markgraf, D. C. F. Wieland, C. J. Sahle, J. Möller, M. Paulus, M. Tolan, and R. Winter, *Phys. Rev. Lett.* **106**, 178102 (2011).
- [16] D. Russo, M. G. Ortore, F. Spinozzi, P. Mariani, C. Loupiac, B. Annighofer, and A. Paciaroni, *Biochim. Biophys. Acta, Gen. Subj.* **1830**, 4974 (2013).
- [17] M. G. Ortore, F. Spinozzi, P. Mariani, A. Paciaroni, L. R. S. Barbosa, H. Amenitsch, M. Steinhart, J. Ollivier, and D. Russo, *J. R. Soc. Interface* **6**, S619 (2009).
- [18] M. A. Schroer, Y. Zhai, D. C. F. Wieland, C. J. Sahle, J. Nase, M. Paulus, M. Tolan, and R. Winter, *Angew. Chem., Int. Ed. Engl.* **123**, 11 615 (2011).
- [19] J. Möller, M. A. Schroer, M. Erkkamp, S. Grobelny, M. Paulus, S. Tiemeyer, F. J. Wirkert, M. Tolan, and R. Winter, *Biophys. J.* **102**, 2641 (2012).
- [20] R. C. Neuman, W. Kauzmann, and A. Zipp, *J. Phys. Chem.* **77**, 2687 (1973).
- [21] C. Krywka, C. Sternemann, M. Paulus, M. Tolan, C. Royer, and R. Winter, *Chem. Phys. Chem.* **9**, 2809 (2008).
- [22] N. J. Brooks, B. L. L. E. Gauthe, N. J. Terrill, S. E. Rogers, R. H. Templer, O. Ces, and J. M. Seddon, *Rev. Sci. Instrum.* **81**, 064103 (2010).
- [23] See Supplemental Material at <http://link.aps.org/supplemental/10.1103/PhysRevLett.112.028101> for sample preparation, SAXS measurements and data analysis, additional Figs. S1-S3.
- [24] S. V. G. Menon, V. K. Kelkar, and C. Manohar, *Phys. Rev. A* **43**, 1130 (1991).
- [25] G. A. Vliegthart and H. N. W. Lekkerkerker, *J. Chem. Phys.* **112**, 5364 (2000).
- [26] M. G. Noro and D. Frenkel, *J. Chem. Phys.* **113**, 2941 (2000).
- [27] A. George and W. W. Wilson, *Acta Crystallogr. Sect. D* **50**, 361 (1994).
- [28] H. E. Stanley, *Introduction to Phase Transitions and Critical Phenomena* (Oxford University Press, Oxford, 1971).